The Interaction of Epidermal Growth Factor with Its Receptor in A431 Cell Membranes: A Stopped-Flow Fluorescence Anisotropy Study†

Dennis L. Rousseau Jr.,‡ James V. Staros,*,§ and Joseph M. Beechem*,||

Departments of Biochemistry, Molecular Biology, and Molecular Physiology and Biophysics, Vanderbilt University, Nashville, Tennessee 37232

Received June 13, 1995; Revised Manuscript Received August 29, 1995⊗

ABSTRACT: We describe a quantitative examination of the interaction of epidermal growth factor (EGF) with the EGF receptor using A431 cell membrane vesicles as a receptor source. Using T-format steady-state fluorescence anisotropy detection coupled with stopped-flow mixing, we measured the association and EGF-induced dissociation kinetics of fluorescein 5-isothiocyanate-labeled mEGF (FITC-EGF) with the EGF receptor over a wide range of FITC-EGF concentrations, membrane dilutions, and time scales (milliseconds to minutes). Fluorescence anisotropy-based equilibrium binding titrations were also performed. All studies utilized the same receptor preparation, ligand preparation, and detection system. The entire data surface (≈78 000 data points) was simultaneously analyzed using global analysis techniques with a variety of kinetic models. Our analysis identified with a high level of confidence receptor populations with two association rate constants ($k_{on} = 1.2 \times 10^6$ M^{-1} s^{-1}, 7.2×10^6 M^{-1} s^{-1}) and three dissociation rate constants ($k_{off} = 0.95 \times 10^{-2}$ s^{-1}, 0.13×10^{-2} s^{-1}, 0.32×10^{-3} s^{-1}), which reflect the presence of at least two distinct receptor populations in A431 cell membranes. Analysis of the kinetic data was found to be much more sensitive to the presence of multiple receptor populations than was the analysis of the equilibrium binding data.

Epidermal growth factor (EGF)[1] is a 6 kDa polypeptide hormone which manifests mitogenic activity through binding a 170 kDa receptor (reviewed in Carpenter & Wahl, 1990, and Ullrich and Schlessinger, 1990). Binding of EGF to its receptor stimulates a protein kinase (Carpenter et al., 1979) specific for tyrosyl residues (Ushiro & Cohen, 1980) that is part of the receptor itself (Buhrow et al., 1982, 1983). The structure of the receptor, as predicted from its cDNA-derived sequence, consists of an extracellular, glycosylated, ligand-binding domain, a single transmembrane segment, and an intracellular kinase domain (Ullrich et al., 1984). In addition to activation of the intrinsic kinase activity, binding of EGF triggers receptor dimerization (Yarden & Schlessinger, 1987a,b; Böni-Schnetzler & Pilch, 1987; Cochet et al., 1988; Fanger et al., 1989), clustering of the receptors at the morphological level (Haigler et al., 1978, 1979; Schlessinger et al., 1978; McKanna et al., 1979), and activation of complex signaling pathways which ultimately lead to cell division (see Carpenter & Cohen, 1990; Ullrich & Schlessinger, 1990). EGF activation of the receptor, which includes (Chen et al., 1987; Honegger et al., 1987; Moolenaar et al., 1988) but is not limited to stimulation of the kinase activity (Coker et al., 1994), is required for EGF-mediated signal transduction.

There is also evidence that the EGF receptor can exist in both high and low affinity states and that the biological actions of EGF may be mediated solely though the high affinity receptor population (King & Cautrecasas, 1982; Kawamoto et al., 1983; Defize et al., 1989; Bellot et al., 1990). The nature of the high affinity EGF receptor state is unclear, although some evidence suggests that receptor oligomerization (Yarden & Schlessinger, 1987a,b; Böni-Schnetzler & Pilch, 1987; Zhou et al., 1993), receptor association with cytoplasmic proteins (Walker & Burgess, 1991), and/or receptor association with the cytoskeleton (Wiegant et al., 1986; van Bergen en Henegouwen et al., 1989) may be involved in the modulation of receptor affinity. Because the binding of EGF to the EGF receptor is the initiating step for EGF mitogenic signaling, a detailed examination of this step is important for the complete understanding of the mechanism of EGF signal transduction.

Much of the information on EGF binding and EGF receptor affinity is derived from equilibrium binding studies using ^{125}I-mEGF on a variety of cell types and membrane preparations. These studies, when analyzed by the method of Scatchard (1949), produce a curvilinear plot which has been interpreted as indicative of the presence of two EGF receptor populations which differ in their binding affinity for EGF. In general, these studies show a small population of high affinity EGF binding sites ($K_d \approx 0.1$ nM) and a large population of lower affinity sites ($K_d \approx 1$ nM) (Gill et al., 1987). However, the interpretation of a curvilinear Scatchard plot is not without problems (for discussion, see Carpenter,

† This work was supported in large part by Grant P01 CA43720 from the National Institutes of Health. D.L.R. was supported in part through a fellowship from the Vanderbilt University Medical Scientist Training Program. J.M.B. was a Lucille P. Markey Scholar. A preliminary account of part of this work was presented at the 1993 Biophysical Society annual meeting (Rousseau et al., 1993).

* Correspondence may be addressed to either author.

‡ Department of Biochemistry.

§ Department of Molecular Biology.

|| Department of Molecular Physiology and Biophysics.

⊗ Abstract published in *Advance ACS Abstracts,* October 15, 1995.

[1] Abbreviations: BSA, bovine serum albumin; CMF-PBS, Ca^{2+},Mg^{2+}-free phosphate-buffered saline; DMF, *N,N*-dimethylformamide; EGF, epidermal growth factor; mEGF, murine EGF purified by the method of Savage and Cohen (1972); EGTA, ethylene glycol bis(β-aminoethyl ether)-*N,N,N′,N′*-tetraacetic acid; FITC, fluorescein 5-isothiocyanate; FITC-EGF, fluorescein-labeled mEGF; HEPES, *N*-(2-hydroxyethyl)piperazine-*N′*-2-ethanesulfonic acid; HPLC, high-performance liquid chromatography; $NaDodSO_4$, sodium dodecyl sulfate; TEA, triethylamine; TFA, trifluoroacetic acid; Tris, tris(hydroxymethyl)-aminomethane.

0006-2960/95/0434-14508$09.00/0

1987; Johnson & Frazier, 1985), and an alternative explanation of the curvilinear Scatchard plot in relation to receptor affinity has been offered (Wofsy et al., 1992). Another method used to examine EGF binding is to determine the rate constants by pre-equilibrium binding studies using ^{125}I-EGF (Mayo et al., 1989; Bellot et al., 1990; Waters et al., 1990, and references therein; Berkers et al., 1992). These studies, performed on a number of cell types, reported a variety of association and dissociation rate constants. There are differences among the studies on the number of association and dissociation constants necessary to explain the binding data as well as differences in demonstrating high and low affinity receptor populations. Interpretation of these studies is further complicated by possible ^{125}I-EGF heterogeneity (Carpenter et al., 1975; Kienhuis et al., 1991, 1992), a low data sampling rate over the binding period, and small data sets.

Application of spectroscopic methods to the study of EGF/EGF receptor interactions overcomes many of the difficulties inherent in ^{125}I-EGF binding experiments and allows the direct examination of the rate constants involved in EGF binding. The EGF/EGF receptor system is amenable to biophysical studies due to the high specificity of EGF binding and the large size disparity between EGF and its receptor, as well as the ease of labeling murine EGF (mEGF) with spectroscopic probes (reviewed in Carpenter & Wahl, 1990). Because of the large difference in size between EGF and its receptor, receptor binding would be expected to greatly decrease the rotational motion of EGF. As a result, biophysical methods sensitive to the change in the rotational motion of a labeled mEGF molecule could be used to monitor the binding and dissociation kinetics of EGF in real time after rapid mixing. EPR spectroscopy and fluorescence spectroscopy are two such methods. The utility of EPR spectroscopy to examine the dissociation of a spin-labeled mEGF derivative from the EGF receptor in soluble receptor preparations was demonstrated by Faulkner-O'Brien et al. (1991). However, time resolution and sensitivity constraints make examination of the association of the spin-labeled mEGF with its receptor difficult. The utility of fluorescence spectroscopy to examine both the association and dissociation of a fluorescein 5-isothiocyanate-labeled mEGF derivative (FITC-EGF) from its receptor in intact cells was demonstrated by Carraway and Cerione (1993). The study showed that changes in the fluorescence anisotropy of FITC-EGF provided a sensitive measure for the association and dissociation of EGF with the EGF receptor. However, a detailed analysis of the kinetics was not undertaken. To our knowledge, no stopped-flow studies of EGF interaction with EGF receptor using optical methods have been published.

In this report, we described the synthesis and purification of a homogeneous preparation of FITC-EGF, the biological and spectroscopic characterization of this product, and its application in real time measurements of EGF receptor interaction. Using a T-format, steady-state fluorometer mounted on a stopped-flow instrument, we measured in real time the association and dissociation of FITC-EGF with the EGF receptor in A431 cell membrane vesicles after rapid mixing by following the change in steady-state anisotropy of FITC-EGF as it binds to or dissociates from the EGF receptor. The data were subjected to global analysis (Beechem, 1992) using several binding models to derive the rate constants which best describe the observed ligand/receptor interactions. These results were then compared to steady-state anisotropy measurements of EGF binding carried out under equilibrium conditions. Our results indicate that two association rate constants and three dissociation rate constants are necessary to model the real time binding of FITC-EGF to the EGF receptor in membrane vesicles, suggesting the presence of at least two affinity classes of EGF receptors in the membrane preparation. The kinetic experiments were far more sensitive than the equilibrium binding experiments to the presence of the two (or more) affinity classes.

MATERIALS AND METHODS

Murine EGF (mEGF) was prepared as previously described (Savage & Cohen, 1972); ^{125}I-mEGF was prepared by the method of Carpenter and Cohen (1976). Membrane vesicles from A431 cells (Giard et al., 1973; Fabricant et al., 1977; Haigler et al., 1978), in which the EGF receptor is predominantly in the native 170 kD form, were prepared by modifications of the method of Cohen et al. (1982) (see supporting information for details). [γ-^{32}P]ATP (3000 Ci/mmol) was from NEN. HPLC solvents were from Burdick and Jackson. TFA (HPLC grade) and TEA (Sequanal grade) were from Pierce. Fluorescein 5-isothiocyanate (FITC) was from Molecular Probes (F-1906). All aqueous solutions were prepared using water purified with a Mill-Q water system (Millipore). All buffers and salts were purchased from Sigma. DMF (certified ACS) was from Fisher.

Synthesis and Quantitation of Fluorescein-Labeled mEGF (FITC-EGF). mEGF (400 μg) was desalted on a 1 × 8 cm P-2 (Bio-Rad) gel filtration column equilibrated with 50 mM HEPES/100 mM NaCl, pH 7.4, for buffer exchange. This step removed any residual ammonium ions from the mEGF purification. The fraction containing the mEGF was collected and lyophilized. Recovery of mEGF was estimated to be 85−90%. For labeling, a 50-fold molar excess of FITC was dissolved in 360 μL of DMF + 85 mM TEA. This was then added directly to the dry mEGF to start the labeling reaction. The reaction mixture was placed in the dark, and the reaction proceeded for 2−3 h at room temperature. Following the incubation period, the reaction volume was doubled with the addition of 360 μL of 50 mM HEPES/100 mM NaCl, pH 7.4, and any insoluble material was pelleted by centrifugation for 5 min at 14 000 rpm, room temperature, in a microfuge (Eppendorf). Unreacted FITC and the organic solvents were then separated from the labeled and unlabeled mEGF by gel filtration on a 1.6 × 5 cm P-2 column equilibrated with 50 mM HEPES/100 mM NaCl, pH 7.4.

The reaction products in the excluded volume from the P-2 column were purified by reversed-phase HPLC (RP-HPLC) using a 4.6 × 220 mm Brownlee Aquapore RP-300 C-8 cartridge with 0.1% TFA in water (buffer A) and 0.1% TFA in 80:20 AcCN/water (buffer B) as mobile phases. The solvent delivery system consisted of two Waters 510 pumps, and absorbance was monitored at 220, 280, and 440 nm with a Waters 490E programmable multiwavelength detector. The system was controlled from a Maxima 820 workstation. For each HPLC run, the system was equilibrated with 85:15 buffer A/B and loaded with 400−500 μL of the excluded volume. Products were eluted with a 70 min linear gradient of 15−50% buffer B at a flow rate of 1 mL/min. The major peaks with 220, 280, and 440 nm absorbance were hand-collected, lyophilized, redissolved in 1 mL of 20 mM HEPES, pH 7.4, and reinjected using the same HPLC

conditions. The purified products were collected, lyophilized, and redissolved in 20 mM HEPES, pH 7.4. Products were then aliquoted into 500 μL tubes and stored at −75 °C. Purity of the final product was determined by semimicrobore RP-HPLC using a 2.1 × 220 mm Brownlee Aquapore RP-300 C-8 cartridge and the same mobile phases. For these separations, the system was equilibrated with 85:15 buffer A/B, and samples were eluted with a 70 min linear gradient of 15−55% buffer B at a flow rate of 0.4 mL/min.

Since mEGF is normally quantitated using a calculated extinction coefficient of 18 700 M^{-1} cm^{-1} at 280 nm (Taylor et al., 1972), it was necessary to determine the relative contribution of the added FITC label to the 280 nm absorbance. A Spex Fluorolog fluorometer was modified so that both absorbance and excitation spectra could be acquired for a sample of FITC-EGF (details may be found in the supporting information).

The stoichiometry of labeling was also examined by measuring the A_{491} of a 1 mL sample of FITC-EGF in 100 mM Tris, pH 8.0, and quantitating using an extinction coefficient of 84 000 M^{-1} cm^{-1} at 491 nm for fluorescein, determined from a standard solution of a highly purified fluorescein standard (Molecular Probes) dissolved in 100 mM Tris, pH 8.0. These measurements were made using a Cary 1E spectrophotometer and a 1 mL fluorescence cuvette (Hellma).

Biological Characterization of FITC-EGF. The biological activity of FITC-EGF was determined by assaying its ability to compete with ^{125}I-mEGF for EGF receptor binding, to stimulate EGF receptor autophosphorylation, and to stimulate EGF receptor dimerization. The ability of FITC-EGF to compete with ^{125}I-mEGF for EGF receptor binding relative to mEGF was determined in binding assays using A431 cells following general binding assay methods described in Carpenter (1985). A431 cells, grown to confluence in 12-well plates (Costar), were washed two times with 1 mL of prewarmed Hank's balanced salt solution (Sigma). A third wash of 1 mL of Hank's solution was then added, and the plates were cooled on ice for 20 min. Each data point determination used four wells: three wells to determine the degree of competition and one well to correct for nonspecific binding. Nonspecific binding was determined at each data point by preblocking binding sites with a 100-fold excess of unlabeled mEGF. At the start of the assay, the third wash of Hank's solution was removed, and 0.5 mL of binding medium (Dulbecco's modified Eagle medium supplemented with 0.2% BSA) containing 50 ng of ^{125}I-mEGF (10 000 cpm/ng) and 0, 25, 50, 100, 150, or 200 ng of mEGF was added to four wells. In a parallel set of wells, the same additions were made except that FITC-EGF replaced mEGF. Plates were incubated 2 h at 4 °C, and then the wells were washed four times with 1 mL of ice-cold Hank's balanced salt solution supplemented with 0.1% BSA. After the final wash, the contents of the well were solubilized by the addition of 1 mL of 1 N NaOH and incubation at 37 °C for 1 h. Contents of each well were transferred into counting tubes and counted on a Gamma 4000 (Beckman).

For EGF receptor autophosphorylation assays, A431 membrane vesicles were diluted 20-fold with 20 mM HEPES/40 mM NaH_2PO_4, pH 7.4. At the start of the assay, 4 μL of FITC-EGF (16 μM stock) or unlabeled mEGF (16 μM stock) was added to 100 μL of membrane vesicle suspension. Samples were then incubated for 10 min at room temperature and were cooled on ice for 5 min. EGF receptor autophosphorylation was started by adding 72 μL of samples to 8 μL of 10× phosphorylation buffer to give final phosphorylation buffer concentrations of 20 mM HEPES, pH 7.4, 5 mM $MgCl_2$, 1 mM $MnCl_2$, 0.1 mM sodium orthovanadate, and 25 μM ATP with 3 μCi of [γ-^{32}P]ATP per assay. Autophosphorylation proceeded for 3 min on ice. A 35 μL aliquot of this reaction was then quenched by the addition of 25 μL of 4× electrophoresis sample buffer (4× sample buffer: 0.25 M Tris, pH 6.8, 8% $NaDodSO_4$, 40% glycerol, 20% β-mercaptoethanol, and 0.008% bromophenol blue) and heating in a 95 °C heating block for 10 min. After cooling to room temperature, samples were diluted to a final 100 μL volume with water and analyzed by $NaDodSO_4$−PAGE and autoradiography.

The ability of FITC-EGF to stimulate EGF receptor dimerization was examined using solubilized EGF receptor from A431 cells. Cells were solubilized following the method of Fanger et al. (1989) with the substitution of 1% $C_{12}E_8$ for 1% Triton X-100 as the detergent. Dimerization assays were performed as described in Fanger et al. (1989).

$NaDodSO_4$−PAGE and Western Blot Analysis. $NaDodSO_4$−PAGE was performed according to the method of Laemmli (1970) using 4−10% linear gradient separating gels and 4% stacking gels. Electrophoretic transfer of proteins to nitrocellulose (Schleicher & Schuell) was carried out with a Sartoblot II (Sartorius) semidry transfer apparatus according to the manufacturer's instructions using a current of 4 mA/cm^2 for 25 min. Immunostaining of the transferred proteins was carried out using the Bio-Rad Immun-Blot goat anti-rabbit alkaline phosphatase assay kit (Bio-Rad) following the manufacturer's instructions. The primary antibody was anti-EGF receptor antiserum from rabbit (gift of Professor Stanley Cohen).

Time-Resolved Fluorescence Measurements of FITC-EGF. The L-format, time-resolved fluorometer has been described in detail elsewhere (Bloom et al., 1994; Perez-Howard et al., 1995). The typical impulse response functions for the system were 60−80 ps (full width at half-maximum amplitude). The fluorescence spectra of FITC-EGF were acquired from a 150 μL sample of 1 μM FITC-EGF in 20 mM HEPES, pH 7.4, in a 3 mm path length cuvette thermostated to 20 °C. The excitation wavelength was 306 nm, and the emission monochromator was set at 520 nm. The emission polarizer was rotated between the vertical and horizontal position every 30 s during the acquisitions (ISS Koala unit, Urbana, IL). Each data set consists of the signal averaged data from 30 30-s acquisitions of the vertically or horizontally polarized emissions. The instrument G factor was determined by rotating the excitation beam to the horizontal position and acquiring a data set of signal-averaged data from 15 30-s acquisitions of vertically or horizontally polarized emission. An impulse response data set was acquired using a 20 mM HEPES, pH 7.4, buffer blank sample with the emission monochromator set at 315 nm. Correlation times for FITC-EGF were determined by simultaneously fitting the vertically and horizontally polarized emission spectra from FITC-EGF using the Globals Unlimited software package (Globals Unlimited, Urbana, IL) (Beechem et al., 1991).

Determination of Comparative Fluorescence Quantum Yield for Free and Receptor-Bound FITC-EGF. Change in the fluorescence quantum yield of FITC-EGF after EGF receptor binding was determined by comparing the emission spectra of bound and free FITC-EGF. Emission spectra were acquired using a Spex Fluorolog fluorometer with the

excitation wavelength set at 470 nm and the emission monochromator scanned from 490 to 600 nm. To decrease scattered light, both a 480 and a 500 nm cut-on filter were placed in front of the emission monochromator. To determine the emission spectrum of bound FITC-EGF, a 1 mL sample of 100-fold diluted A431 membrane vesicles (receptor concentration ~30 nM) was preincubated with 5 μL of 20 mM HEPES, pH 7.4, for 5 min at room temperature in a 1 mL fluorescence cuvette (Hellma). A background scan was made of the sample, and then 5 μL of 1 μM FITC-EGF was added, mixed, and allowed to incubate for 4−5 min at room temperature. The sample was then rescanned, and the background was subtracted. To determine the emission spectrum of unbound FITC-EGF, a similar sample of A431 membrane vesicles was preincubated with 5 μL of 165 μM mEGF to block all binding sites. A background spectrum was taken from this sample; FITC-EGF was added, and the sample was rescanned. From both bound and unbound FITC-EGF, the experiment was repeated three times, and the resulting spectra were averaged. The averaged spectra for bound and unbound FITC-EGF were integrated, and the integration values were compared to evaluate any change in the quantum yield.

Real-Time Measurement of FITC-EGF Binding to the EGF Receptor in A431 Membrane Vesicles. A T-format, steady-state fluorometer for monitoring the rapid anisotropy change in FITC-EGF upon binding was utilized, as described in Otto et al. (1994) and Perez-Howard et al. (1995). An Innova Model 304 argon ion laser (Coherent), tuned to 488 nm and operated in the light regulation mode, was used as the light source. The rapid-mixing module consisted of a SFM-3 stopped-flow unit (Molecular Kinetics, Pulman, WA) equipped with an FC.15 fluorescence cuvette (35 μL) and a hard-stop shutter. Sample mixing was carried out at a 1 mL/s flow rate, which resulted in a nominal dead time of ~15 ms. (For further details concerning this instrument, please see the supporting information.)

The temperature of all reagents in the stopped-flow syringe unit was maintained at 20 °C by a circulating water bath. In FITC-EGF binding experiments, 150 μL of FITC-EGF stocks and 150 μL of A431 membranes (prepared as described above) were mixed to give final FITC-EGF concentrations of 1, 2.5, 5, 10, 20, 40, and 80 nM and a final A431 membrane vesicle dilution of 100-fold. At 5 and 20 nM FITC-EGF concentrations, membrane dilution binding experiments were also performed using the same mixing volumes to give final membrane dilutions of 200-fold at 5 nM FITC-EGF and 200- and 400-fold at 20 nM FITC-EGF. In control experiments, the A431 membranes were preincubated with 1 μM unlabeled mEGF (final concentration) before the stopped-flow mixing with FITC-EGF. For each FITC-EGF concentration and each membrane dilution, the mixing experiment was repeated 10 times, and the data from each mix were added together for the final experimental data set for that concentration or dilution. Background counts were measured for each data set by mixing 150 μL of A431 membranes with 150 μL of 20 mM Hepes, pH 7.4. Each experimental data set was corrected for background, and the vertically and horizontally polarized emission intensities were transformed to anisotropy values using the formula:

$$r = \frac{(I_{\parallel}G) - I_{\perp}}{(I_{\parallel}G) + (2I_{\perp})} \quad (1)$$

The anisotropy data were then smoothed using a running average function with a window of 10 data points (100 ms). The smoothed data sets were then analyzed by global analysis fitting of the data using a nonlinear least squares method (Beechem, 1992). The recovered rate constants were independent of this smoothing window. For global analysis, a linked exponential model, a one binding site model, or a two binding site model was utilized in the fitting routine. The rate equation used for the one site model was:

$$\frac{d[\text{FITC-EGF}_{\text{bound}}]}{dt} = k_{\text{on}}[\text{FITC-EGF}_{\text{free}}][\text{EGFR}] - k_{\text{off}}[\text{FITC-EGF}_{\text{bound}}] \quad (2)$$

The rate equation for the two site model was:

$$\frac{d[\text{FITC-EGF}_{\text{bound}}]}{dt} = [\text{FITC-EGF}_{\text{free}}](k_{\text{on1}}[\text{EGFR}_1] + k_{\text{on2}}[\text{EGFR}_2]) - (k_{\text{off1}}[\text{FITC-EGF}_{\text{bound1}}] + k_{\text{off2}}[\text{FITC-EGF}_{\text{bound2}}]) \quad (3)$$

For each model, the observed anisotropy was calculated from the concentrations of the individual species using the formula:

$$r_{\text{measured}} = (r_{\text{free}}[\text{FITC-EGF}_{\text{free}}]) + (r_{\text{bound}}[\text{FITC-EGR}_{\text{bound}}]) \quad (4)$$

Because the relative quantum yields of bound and free FITC-EGF, determined as described above, were identical (data not shown), it was not necessary to include a quantum yield term in this equation. The value for r_{free} was determined from the control experiments to be 0.085 ± 0.005; the value for r_{bound} was determined to be ~0.20. Its exact value was determined during the nonlinear fitting. The differential rate equations for each of these models were solved using the method of finite difference in a subroutine incorporated into a global analysis kernel (Globals Unlimited, Urbana, IL).

Measurement of Ligand-Induced FITC-EGF Dissociation from EGF Receptor in A431 Membrane Vesicles. The rate of EGF-induced FITC-EGF dissociation from EGF receptor in A431 membrane vesicles was determined using both the stopped-flow steady-state fluorometer described above and, for longer dissociation experiments, a T-format steady-state fluorometer using the same excitation and emission equipment built around a standard cuvette holder. All experiments were done at 20 °C. For the stopped-flow experiments, 50-fold diluted A431 membrane vesicles were preincubated with 20 nM FITC-EGF for 5 min at room temperature before loading into the stopped-flow. To measure dissociation, 150 μL of membranes with FITC-EGF prebound was mixed with 150 μL of 2 μM unlabeled mEGF in 20 mM HEPES, pH 7.4. Final FITC-EGF concentration was 10 nM. For control experiments, 150 μL of membranes with FITC-EGF prebound was mixed with 150 μL of 20 mM HEPES, pH 7.4, in the absence of unlabeled mEGF. Background measurements for each experiment were made by mixing 150 μL of membranes without prebound FITC-EGF with 150 μL of 2 μM unlabeled mEGF in 20 mM HEPES, pH 7.4. Data were acquired at 500 ms intervals, which allowed 78 min of dissociation data to be collected per experiment. For observations longer than 80 min, the stopped-flow apparatus proved unsatisfactory due to problems with vesicle settling and photobleaching. Therefore, long term dissociation experiments were performed using the fluorometer built

around a standard cuvette holder, a 3 mL, 1 cm path length cuvette (Hellma), and continuous stirring during the time course of the experiments. In the long dissociation experiments, FITC-EGF was prebound to membranes in 2 mL of 20 mM HEPES, pH 7.4, in the sample cuvette. At the start of the dissociation experiment, 1 mL of unlabeled mEGF in 20 mM HEPES, pH 7.4, was rapidly hand-mixed into the cuvette. This addition resulted in a final membrane dilution of 100-fold, and a final unlabeled mEGF concentration of 2 μM. Final FITC-EGF concentrations examined were 5, 10, and 20 nM. For control experiments, 1 mL of 20 mM HEPES, pH 7.4, was added to the FITC-EGF/membrane sample. Background measurements were made using 3 mL of 100-fold diluted membranes in 20 mM HEPES, pH 7.4. Data were acquired at 2 s intervals, allowing 270 min of dissociation data per experiment; the time delay from hand-mixing to data collection was 6−10 s. All experimental and control data sets were corrected for background and transformed to anisotropy values using eq 1. The dissociation data sets were fit in a linked exponential analysis using a nonlinear least squares method (Beechem, 1992) in the global analysis software.

Error Analysis. Error analysis of all fitting parameters was performed using the exhaustive search method (Beechem et al., 1991, and references therein). To obtain the asymmetric standard deviation associated with the fitting parameter, the *F*-statistic criterion (Johnson & Frasier, 1985) was utilized to determine a statistically significant increase in χ^2. The parameter values on either side of the fitting minimum associated with the significant χ^2 values represent the standard deviation for that fitting parameter. All programs for the nonlinear least squares analysis were written in Fortran 77 using the Lahey (F77L/EM32, Incline Village, NV) Fortran compiler running in the 32-bit protected mode and were run on an Intel 486DX-based microcomputer.

Equilibrium Binding of FITC-EGF with the EGF Receptor in A431 Membrane Vesicles. For equilibrium binding experiments, a standard cuvette holder replaced the stopped-flow apparatus in the T-format steady-state fluorometer. All measurements were made at room temperature using a 1 mL, 1 cm path length fluorescence cuvette (Hellma). In a complete equilibrium binding experiment, 1 mL of 100-fold diluted A431 membrane vesicles was loaded into the cuvette. Increasing concentrations of FITC-EGF were then added to the membranes; the sample was allowed to equilibrate for 5 min; and then the counts/s for vertically and horizontally polarized emission were measured for 30 s using a 1 s sampling rate. At each FITC-EGF concentration, the counts over the 30 s measurement were then totaled and corrected for background, and the final anisotropy values were used for the $I_{\parallel}$ and $I_{\perp}$ variables in eq 1. With this method, equilibrium anisotropy values were measured for 0.7, 1.5, 3, 4.5, 6, 9, 12, 16, 21, 25, 29, 44, 59, 88, 117, 160, and 200 nM FITC-EGF (final concentrations). In control experiments, the membrane vesicles were preincubated with 1.6 μM unlabeled mEGF for 10 min prior to addition of increasing concentrations of FITC-EGF. In all experiments, the total volume change of the membrane sample never exceeded 5% after all additions. The concentration of EGF receptor in the A431 membrane vesicles and the dissociation constant (K_d) for the FITC-EGF/EGF receptor complex were determined from an anisotropy versus [FITC-EGF] plot by nonlinear analysis using Weber's (1992) solution of:

$$K_d = \frac{(R_0 - [RL])(L_0 - [RL])}{[RL]} \quad (5)$$

where R_0 is the total EGF receptor concentration, L_0 is the total FITC-EGF concentration, and [RL] is the concentration of FITC-EGF/EGF receptor complex. Both single affinity and two affinity receptor population models were used to determine the best-fit binding parameters.

RESULTS AND DISCUSSION

Synthesis and Quantitation of FITC-EGF. The utility of fluorescein-labeled mEGF in the study of receptor binding kinetics has been demonstrated (Rousseau et al., 1993; Carraway & Cerione, 1993). In the Carraway and Cerione (1993) study, binding of an FITC-labeled EGF preparation to the receptor was detected by changes in fluorescence anisotropy after hand-mixing of the fluorescent ligand with a suspension of A431 cells. Hand-mixing necessarily limits the information that can be obtained at short times after introduction of the ligand. Whether because of this limitation in the data or for some other reason, results of these experiments were analyzed assuming a single class of binding sites.

In order to undertake a more detailed kinetic analysis of EGF/EGF receptor interaction using fluorescence measurements, it was important to develop methods for producing an FITC-labeled mEGF species that was homogeneous, biologically indistinguishiable from unlabeled mEGF, and well characterized biophysically. Given the highly reactive nature of the isothiocyanate moiety, it would not be unexpected to form a number of labeled mEGF products in the FITC/mEGF reaction. The multiple products formed in the anhydrous reaction of FITC with mEGF are shown in Figure 1A, which is an HPLC chromatogram of the FITC/mEGF reaction mixture following P-2 gel filtration. Two predominant product peaks are seen at 58 and 61 min. Under the same HPLC conditions, unlabeled mEGF elutes at 49.5 min. For further purification, these two products were hand-collected, lyophilized, redissolved in 20 mM HEPES, pH 7.4, and reinjected using the same HPLC method. Both purified products were assayed for their ability to stimulate EGF receptor autophosphorylation (see below). Since we were interested in obtaining a single labeled product with the highest yield, we focused our further efforts on the product in the 58 min peak. Purity of this product was assessed by semi-microbore RP-HPLC; the HPLC chromatogram of the final purified product is seen in Figure 1B.

Addition of the fluorescein label to mEGF complicated the precise quantitation of the FITC-EGF in solution. Use of fluorescence and/or absorbance measurements of the FITC-EGF as compared to known FITC or fluorescein standards could result in significant errors in quantitation, as it is unknown what effect the labeling of mEGF with FITC has on the absorbance and fluorescence properties of the fluorescein. There is also the possibility of a multiply labeled product. Use of the A_{280} of FITC-EGF compared to the known A_{280} of mEGF would result in significant error in quantitation as the fluorescein moiety would be expected to increase the A_{280} of mEGF. Our method of quantitation focused on separating the relative contribution of the fluorescein and the mEGF molecule to the overall A_{280} of FITC-EGF. The absorbance and normalized excitation spectra are shown in Figure 2. Because the signal in the

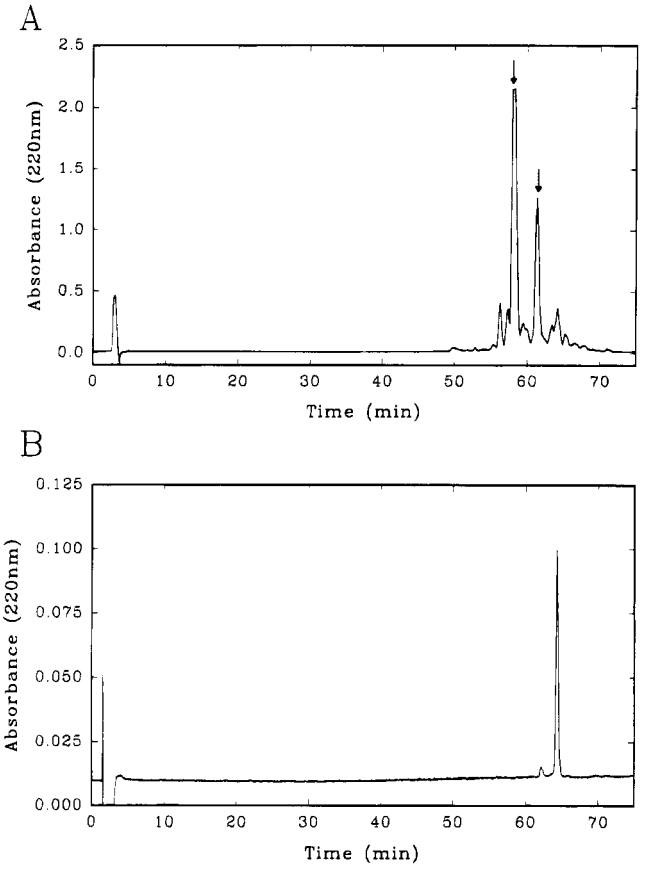

FIGURE 1: RP-HPLC purification of FITC-EGF. Panel A is the A_{220} chromatogram of a preparative separation of the FITC-EGF synthesis reaction following P-2 gel filtration. The peaks at 58 and 61 min (arrows) had EGF biological activity as assessed in EGF receptor autophosphorylation assays. The product in the 58 min peak was used in all subsequent experiments. Panel B is the A_{220} chromatogram of the semi-microbore RP-HPLC experiment assessing the purity of the final FITC-EGF product.

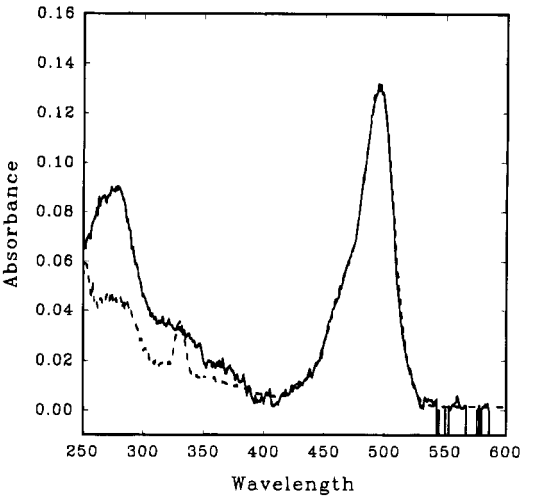

FIGURE 2: Determination of fluorescein contribution to the A_{280} of FITC-EGF. This plot represents the absorption (—) and normalized emission spectra (- - -) used to determine the 280 nm absorbance contribution of the fluorescein label. The data were acquired as described in Materials and Methods. The total A_{280} of FITC-EGF was 0.090. Since all absorbance in the normalized emission spectrum is due to the fluorescein label, its relative contribution to the total A_{280} can be determined from this plot. The data indicate that $A_{280} = 0.044$ was contributed by the fluorescein label and $A_{280} = 0.046$ was contributed by mEGF. Using $\epsilon_{280} = 18\,700\ M^{-1}\ cm^{-1}$ (Taylor et al., 1972) for mEGF, the concentration of mEGF in the FITC-EGF sample could then be quantitated.

excitation spectrum results from the fluorescein label only, its value in the normalized spectrum at 280 nm represents the contribution of the label to the overall A_{280} of the FITC-EGF molecule. The total A_{280} for the sample was 0.090. From the normalized emission spectrum, it was determined that the fluorescein contributed an A_{280} of 0.044 to the total absorbance, leaving 0.046 as the A_{280} contribution of mEGF. Using $\epsilon_{280} = 18\,700\ M^{-1}\ cm^{-1}$ for mEGF and correcting for dilution, the concentration of EGF in the FITC-EGF stock was then determined. Based on our measurements, FITC-EGF has an $\epsilon_{280} = 36\,000\ M^{-1}\ cm^{-1}$. Based on the final quantitation, yields of the labeling reaction ranged from 25% to 40%. The stoichiometry of labeling was determined from the A_{491} of the quantitated FITC-EGF, using $\epsilon_{491} = 84\,000\ M^{-1}\ cm^{-1}$ for fluorescein, determined using a high purity fluorescein standard (Molecular Probes). From these results, the labeling stoichiometry was calculated to be 0.95 mol of fluorescein/mol of EGF.

Biologial Characterization of FITC-EGF. The ability of both FITC-EGF products (58 and 61 min peaks) and mEGF to stimulate EGF receptor autophosphorylation was compared in autophosphorylation assays using EGF receptor in A431 membrane vesicles. The results of this experiment are seen in Figure 3A. The result suggests that both FITC-EGF products stimulate receptor autophosphorylation to a degree similar to that of unlabeled mEGF. Based on the spectroscopic absorbance patterns of each product (data not shown), it appears that each is a singly labeled FITC-EGF. That each product has a different retention time by HPLC suggests that the label is located in a different position on mEGF. The mEGF molecule has two sites, the amino terminus and His22, which might react with the isothiocyanate group of FITC. Interestingly, mutation of the His22 to Tyr22, tyrosine being the residue in this position in human EGF, and reaction of this product with FITC yield a chromatogram in which the second peak is absent (R. A. Stein, D. L. Rousseau, Jr., C. A. Guyer, and J. V. Staros, unpublished results). This suggests that the FITC-EGF product in the 58 min peak represents mEGF with the FITC label at the amino terminus. Because the 58 min peak product was the dominant FITC-EGF species, all further characterization efforts were focused on it alone. For the remainder of this paper, FITC-EGF will refer to this product.

FITC-EGF and mEGF were compared in their relative abilities to compete with ^{125}I-mEGF for receptor binding using A431 cells in a competitive binding assay based on general binding assay methods described in Carpenter (1985). Figure 3B shows that FITC-EGF and mEGF are comparable in their abilities to compete with ^{125}I-mEGF for receptor binding. Finally, both FITC-EGF and mEGF were shown to be comparable in their ability to induce dimerization of solubilized EGF receptor (Rousseau, 1993) using cross-linking methods described in Fanger et al. (1989). Taken as a whole, these studies suggest that the FITC-EGF and mEGF are indistinguishable, within the limits of these experiments, in their abilities to compete for receptor binding, stimulate receptor autophosphorylation, and induce receptor dimerization.

Time-Resolved Fluorescence Anisotropy Measurements of FITC-EGF. For spectroscopic characterization, we used time-resolved fluorescence anisotropy measurements to determine the motion of the fluorescein label relative to that of the mEGF molecule. Close coupling of the motion of the fluorescein to that of mEGF is important for the

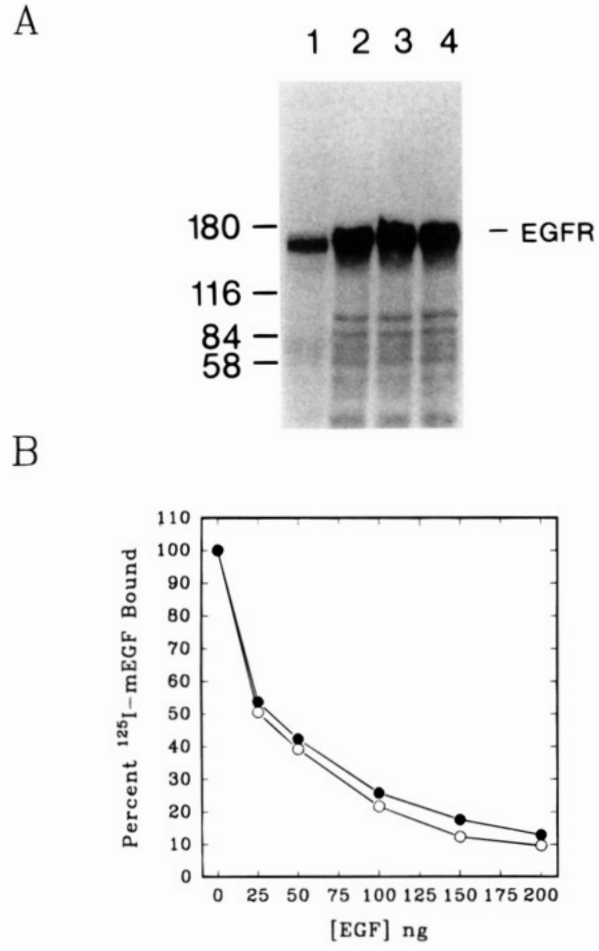

FIGURE 3: Biological characterization of FITC-EGF. Panel A is an autoradiogram of an EGF receptor autophosphorylation assay using A431 cell membrane vesicles as a receptor source. Basal autophosphorylation (lane 1) and autophosphorylation stimulated by addition of 0.6 μM unlabeled mEGF (lane 2), 0.6 μM FITC-EGF (58 min peak, see Figure 1A) (lane 3), and ≈0.6 μM FITC-EGF (61 min peak, see Figure 1A) (lane 4). Autophosphorylation assays were performed as described in Materials and Methods. Samples were separated by $NaDodSO_4$−PAGE (Laemmli, 1970) using a 4−10% gradient gel. The autoradiogram was produced by a 2−3 h exposure of the dried gel on Kodak XAR-5 film. Panel B shows the comparison of the ability of unlabeled mEGF (○) and FITC-EGF (●) to compete with ^{125}I-mEGF for EGF receptor binding on A431 cells. In this assay, 0, 25, 50, 100, 150, and 200 ng of competing mEGF was added with 50 ng of ^{125}I-mEGF (10 000 cpm/ng) to A431 cells in 12-well plates. Following incubation for 2 h on ice, the cells were washed extensively, solubilized with 1 N NaOH, and counted. Nonspecific binding at each concentration was determined by the preaddition of a 100-fold excess of unlabeled wt mEGF and was always less than 10%. Each data point was determined in triplicate, and the resulting values were corrected for nonspecific binding and then averaged. The percent ^{125}I-mEGF bound was calculated by dividing the specific bound counts at each concentration of competing EGF by the specific bound counts of ^{125}I-mEGF in the absence of competing mEGF.

sensitivity of the association and dissociation studies, since the magnitude of the change in steady-state anisotropy caused by FITC-EGF binding to receptor is, in part, determined by how closely the motion of the probe reflects that of the protein. Figure 4 shows the time-resolved fluorescence anisotropy measurement of FITC-EGF in aqueous buffer at 20 °C. The excitation wavelength of 306 nm excited fluorescein in its negative transition for anisotropy measurements, so the anisotropy decays toward zero. Figure 4 (upper panel) shows the anisotropy decay data for FITC-EGF and a fit determined using an anisotropic rotational model. Using

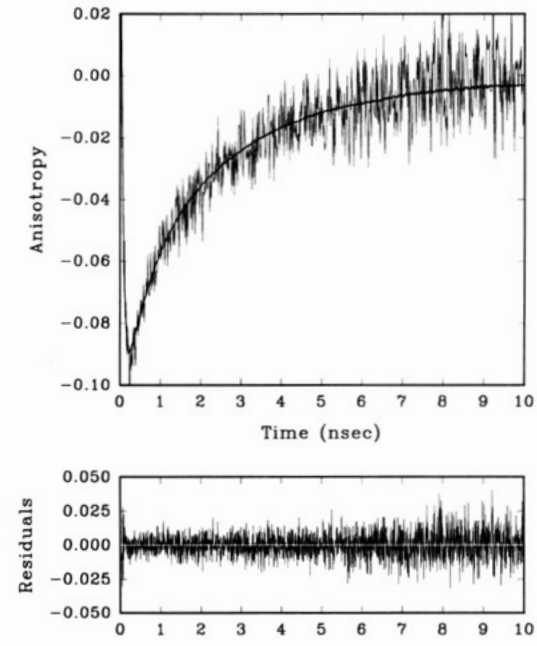

FIGURE 4: Time-resolved fluorescence anisotropy decay of FITC-EGF. The upper panel represents the anisotropy decay data for FITC-EGF in aqueous buffer at 20 °C. Because the excitation wavelength of 306 nm excited the fluorescein molecule in its negative anisotropy transition, the spectrum begins at a negative anisotropy and decays toward zero. The vertically and horizontally polarized emission spectra which generated the anisotropy data were fit to both isotropic and anisotropic rotational models using global analysis software (Globals Unlimited, Urbana, IL). Fitting with the isotropic model returned two lifetimes of $\tau = 3.6$ ns ($\alpha = 82\%$) and $\tau = 1.1$ ns ($\alpha = 18\%$) with a mean correlation time of $\phi = 2.0$ ns (1.8, 2.2; SD). Using the anisotropic model, the lifetimes remained unchanged and the mean correlation time was divided into two correlation times of 0.63 ns (0.15, 1.5; SD) ($\beta = -0.033$) and 2.66 ns (2.1, 6.4; SD) ($\beta = -0.067$). The fit for the anisotropic model is shown with the anisotropy decay data; the residuals of the fit are shown below.

an isotropic rotational model, the mean single correlation time recovered was 2.0 ns (1.8, 2.2; SD) (data not shown). A statistically better fit (Figure 4) was generated using an anisotropic rotational model (ellipsoid) with two correlation times. The resulting correlation times from this fit were 0.63 ns (0.2, 1.5; SD) ($\beta = -0.033$) and 2.66 ns (2.1, 6.4; SD) ($\beta = -0.067$). These values are in good agreement with previously reported values of 0.55 and 4 ns at 20 °C (Ghiron et al., 1992) for human EGF using the intrinsic tryptophan fluorescence. The nature of the two rotational correlation times is unclear. Ghiron et al. (1992) attributed the 4 ns correlation time to the global motion of EGF and the 0.55 ns correlation time to local tryptophan motion. Our 2.66 ns correlation time could represent the rotation of the mEGF molecule itself, while the 0.63 ns correlation time could represent some fast local motion of the fluorescein probe. However, from the NMR solution structure of mEGF (Montelione et al., 1992; Kohda & Inagaki, 1992), it is known that the mEGF molecule is not spherical, so the two correlation times could represent different rotational motions of the mEGF molecule about different axes. Further experiments would be necessary to distinguish between the two possibilities. However, for the purposes of this study, the absence of any large amplitude fast motion in the anisotropy decay curve indicates that the fluorescein is relatively immobilized on the mEGF molecule. These results suggest that our FITC-EGF is a different species than the FITC-labeled mEGF described in Carraway and Cerione

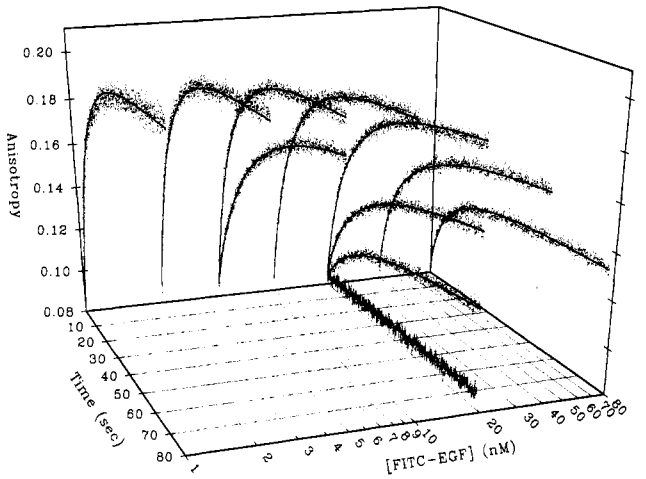

FIGURE 5: Real-time binding of FITC-EGF to the EGF receptor in A431 membrane vesicles. This figure shows the anisotropy vs time plots of the entire FITC-EGF binding data set for all FITC-EGF concentrations and receptor dilutions. The FITC-EGF concentrations used were 1, 2.5, 5, 10, 20, 40, and 80 nM. At the 5 and 20 nM FITC-EGF concentrations, the receptor dilutions of 1:1 (5 nM) and 1:1, 1:3 (20 nM) are also shown. The entire FITC-EGF binding data set represented here consists of 10 spectra of 7835 data points each. For each spectrum in this figure, only every fifth data point is plotted. At the 20 nM FITC-EGF concentration, a representative control experiment is shown in which the EGF receptor sites were preblocked with a 50-fold excess of unlabeled mEGF before the FITC-EGF binding experiment; for this spectrum, every data point is plotted to demonstrate the actual data density acquired in each spectrum. The fit lines represent the results from fitting this data surface with the two site binding model (eq 3). The parameter values recovered in this analysis are shown in Table 2. Comparison of this fit with the linked exponential fit gives a ratio of variance of 1.05. This low ratio of variance as well as the adequate fits of the data suggest that this model provides a good description of FITC-EGF binding to the receptor.

(1993), where the fluorescein moiety was reported to have a significant degree of rotational freedom from that of mEGF.

Real-Time Measurements of the Binding of FITC-EGF to the EGF Receptor in A431 Membrane Vesicles. The anisotropy vs time data for FITC-EGF binding to the EGF receptor on the surface of A431 membrane vesicles using seven FITC-EGF concentrations and three membrane dilutions are shown in Figure 5. A typical control mixing experiment with EGF receptors preblocked with a 50-fold excess of unlabled mEGF is also shown in Figure 5. The control experiments established that preblocking EGF receptors before the binding experiment resulted in no measurable increase in the steady-state anisotropy of FITC-EGF, indicating that observed steady-state anisotropy changes in the binding experiment were due to specific binding of FITC-EGF to the EGF receptor. A variety of analytical approaches were utilized to examine this 78 350 point data surface. Empirical individual or linked exponential global analysis required at least two exponential terms to describe this data surface. The linked exponential analysis resulted in the minimal fitting variance of all of the global analysis models, which was expected, given the large number of independent fitting parameters in the model and the minimal number of constraints imposed on the system. In order to compare different kinetic models, all subsequent model variances were normalized to the minimal fitting variance of the linked exponential model. By this analysis, better fitting models (i.e., lack of systematic deviations in the residual patterns) would have ratios of fitting variances which approach 1.0.

Table 1: One Site Model Fit Using Equation 2

parameter	fit value	std deviation[a] −	std deviation[a] +
k_{on}	2.6×10^6 M^{-1} s^{-1}	2.54	2.65
k_{off}	0.0068 s^{-1}	0.0063	0.0075
[receptor]	28.7 nM	28.3	29.05
r_{bound}	0.213	0.212	0.215
K_d (calcd)[b]	2.6 nM	2.4	3.0

[a] The standard deviation for all parameters was determined using 45 000 degrees of freedom for the analysis. The actual degrees of freedom for this calculation were 78 326, a number which was too large for our statistical software. Therefore, the standard deviations reported will be slightly larger than they actually are. [b] The K_d was calculated from the rate constants fit to the association data. The standard deviation was calculated from the bounds of the individual rate constants, assuming the worst case.

Table 2: Two Site Model Fit Using Equation 3[a]

parameter	fit value	std deviation[b] −	std deviation[b] +
$k_{on}(1)$	1.2×10^6 M^{-1} s^{-1}	1.13	1.30
$k_{off}(1)$	0.004 s^{-1}	0.0033	0.0049
$k_{on}(2)$	7.2×10^6 M^{-1} s^{-1}	6.6	7.8
$k_{off}(2)$	0.001 s^{-1}	−[c]	0.0024
[receptor] (1)	26 nM	25.0	27.5
[receptor] (2)	8.1 nM	7.1	9.1
r_{bound}	0.205	0.2038	0.2060
$K_d(1)$ (calcd)[d]	3.3 nM	2.5	4.3
$K_d(2)$ (calcd)[d]	0.14 nM	−[c]	0.36

[a] The fits to the data using this model are seen in Figure 5. [b] See footnote *a* in Table 1. The actual degrees of freedom for this calculation were 78 323. [c] Lower limit undefined. [d] See footnote *b* in Table 1.

Since the linked exponential model is essentially empirical in nature, it was decided to perform a global analysis directly in terms of the rate constants of the system and the concentrations of the reactants. The results of the global analysis of this data surface in terms of a single EGF receptor class model (eq 2) are shown in Table 1. Comparison of the minimal fitting variance of this model with that of the linked exponential model gave a ratio of variance = 2.05. The large ratio of variance as well as the inadequate fits of the data surface (data not shown) generated by this model allowed rejection of the single site model as an accurate representation of the binding data with a confidence level much greater than 99%. The results of a global analysis of the data in terms of a two EGF receptor class model (eq 3) are shown in Table 2. The fits resulting from these parameters are shown in Figure 5. Comparison of the minimal fitting variance of this model to that of the linked exponential analysis gave a ratio of variance = 1.05. Because the two receptor classes in this model could share an association or dissociation constant, the model was modified to fit the two receptor classes to a single k_{on} and two k_{off}'s (ratio of variance = 1.94) or to two k_{on}'s and a single k_{off} (ratio of variance = 1.05). The single k_{on} model was rejected using the same reasoning used to reject the one site model. The single k_{off} model was not statistically different from the initial two site model. The inability to discern the presence of the second k_{off} term was not unexpected. The k_{off} term for the higher affinity receptor population was not well-defined (see Table 2) in the initial two site model. It is also difficult to delimit a dissociation process with a lifetime in the range of 1000 s from association data alone, which were limited in time to 78.35 s.

Comparing our results to results obtained by other laboratories which examined EGF binding using A431 cell membranes reveals a lack of consensus concerning the presence of one or two affinity populations in the membrane preparations. Using filter binding assays with ^{125}I-mEGF as a ligand, Carpenter et al. (1979) obtained a curvilinear Scatchard plot from equilibrium binding data acquired at 25 °C, which could be interpreted as indicative of the presence of two receptor populations. In contrast, equilibrium binding studies using a filter binding assay and ^{125}I-EGF as ligand (Carraway et al., 1989) or equilibrium binding studies using an FITC-EGF derivative as ligand (Carraway et al., 1990), both performed at room temperature, identified only a single class of EGF receptors in A431 membrane preparations with a K_d = 1.4 nM or 2.4 nM, respectively. In a more detailed analysis, Berkers et al. (1990) studied the equilibrium binding at either 0 °C or room temperature of ^{125}I-EGF with A431 cell membranes prepared by two different methods using a filter binding assay. They reported finding only one population of receptors at either temperature using either membrane preparation. The reported K_d's were 0.63 nM at 0 °C and 0.45 nM at room temperature. These values did not vary significantly between the two membrane preparations. It is also interesting to note that Carraway and Cerione (1993), using anisotropy changes to follow the binding and dissociation of a fluorescein-labeled mEGF derivative, analyzed their data assuming only one class of EGF receptors on the surface of suspended A431 cells.

Our analysis of the binding kinetics clearly supports the presence of at least two receptor populations in A431 cell membrane preparations. However, the nature of these different receptor populations remain unclear. Recent kinetic studies using receptor fragment monomers and dimers in solution suggest that dimeric receptors have higher affinity for EGF as compared to receptor monomers (Zhou et al., 1993), although the difference in affinity was attributed to differences in the k_{off} for the receptor populations. This study did not find significant differences in the k_{on} between monomer and dimer receptor fragments. We have examined cooperativity models as well as models which attributed different receptor affinities to different states of receptor oligomerization (monomer vs dimer). However, since no unique spectroscopic features can be attributed to state of receptor oligomerization, our data lacked any sensitivity to oligomerization parameters which were important to such models. Methods to observe receptor oligomerization in plasma membranes using fluorescent derivatives of mEGF have been developed (Carraway et al., 1989; Azevedo & Johnson, 1990). Future studies combining these methods with the methods presented here may allow determination of the role of receptor oligomerization in the receptor affinity for ligand.

Measurement of Ligand-Induced FITC-EGF Dissociation from EGF Receptor in A431 Membrane Vesicles by Steady-State Anisotropy. Given the inability of the association data to delimit long term dissociation processes, we examined directly the dissociation of FITC-EGF from its receptor in membranes in the presence of a 100-fold excess of unlabeled mEGF. Initial dissociation studies using the stopped-flow instrument demonstrated that this instrument gave reproducible data only for experiments less than 80 min in length and using FITC-EGF concentrations greater than 20 nM. This was primarily due to problems with photobleaching at low FITC-EGF concentrations and vesicle settling in long duration experiments. The hand-mixing instrument with the large cuvette eliminated both of these difficulties. Therefore, dissociation experiments using the stopped-flow were performed using 20 nM FITC-EGF and a total data collection time of 78 min. Hand-mixed dissociation experiments were performed using 5, 10, and 20 nM FITC-EGF with total data collection times of 270 min. Representative anisotropy vs time data for FITC-EGF dissociation from the EGF receptor in A431 membrane vesicles are shown in Figure 6. Independent analysis of the dissociation data at different starting FITC-EGF concentrations failed to reveal concentration-dependent differences in dissociation rates or amplitudes (data not shown). The fits overlaying the data are the results of the global analysis fitting of all dissociation data sets. The nonlinear analysis of the data required three exponential terms to fit the data. The recovered rates for these dissociation processes are as follows: 0.95×10^{-2} s^{-1} (0.78, 1.2; SD), 0.13×10^{-2} s^{-1} (0.12, 0.15; SD), and 0.32×10^{-3} s^{-1} (0.30, 0.33; SD). These rates represent processes with lifetimes of 1.8, 13, and 53 min. The normalized amplitudes of the dissociation processes are 20 ± 7%, 37 ± 7%, and 43 ± 5%, respectively.

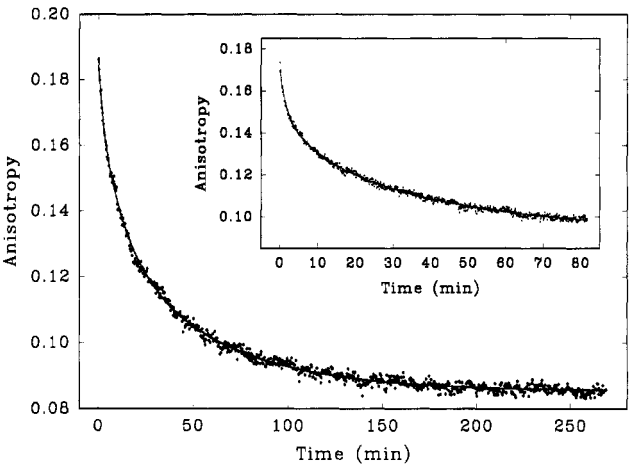

FIGURE 6: Real-time dissociation of FITC-EGF from the EGF receptor in A431 membrane vesicles. The main figure is the anisotropy vs time plot for a hand-mixed dissociation experiment using 10 nM FITC-EGF. The inset figure is the anisotropy vs time plot for a stopped-flow mixed dissociation experiment using 20 nM FITC-EGF. The data shown represent every 10th data point of the actual data set. The fit lines in both plots represent the results of a global analysis of the hand-mixed and stopped-flow mixed experiments. This analysis recovered three dissociation rates of 0.95×10^{-2} s^{-1} (0.78, 1.2; SD), 0.13×10^{-2} s^{-1} (0.12, 0.15; SD), and 0.32×10^{-3} s^{-1} (0.30, 0.33; SD). These rates represent processes with lifetimes of 1.8, 13, and 53 min. The normalized amplitudes of each process are 20 ± 7%, 37 ± 7%, and 43 ± 5%, respectively.

Comparison of the first two dissociation rate constants with the two dissociation constants found in the association experiments (Table 2) shows reasonable agreement between the two (0.004 s^{-1} vs 0.0095 s^{-1}, 0.001 s^{-1} vs 0.0013 s^{-1}). The association experiments were unable to determine the presence of a third dissociation term given its long lifetime. The presence of this third component suggests that there may be more than two affinity classes of the EGF receptor in membrane preparations, at least in the presence of excess EGF. Examination of the amplitudes of each dissociation rate reveals large differences between the populations found in the dissociation experiment as compared to those of the association experiments. In the association experiments, 76% of the receptor population was associated with the larger k_{off},

whereas in the dissociation experiments (unlabeled EGF "chase" experiments) this population dropped to 20%. Populations associated with the smaller k_{off} increased from 24% in the association experiments to a maximum of 80% as seen in the dissociation experiments. The most likely explanation for this difference is that the presence of 100× excess of unlabeled EGF in the chase experiments alters the relative receptor populations in the membranes.

The association experiments allow direct observation of the initial FITC-EGF/EGF receptor interactions, providing information regarding the state of the receptor populations in the absence of EGF. The dissociation experiments are performed in the presence of a large excess of EGF, providing dissociation information only for fully saturated receptor populations without regard to the starting concentration of FITC-EGF. The distinct nature of the association and dissociation experiments argues against simplistically combining the data to obtain discrete equilibrium binding constants. However, both sets of data support the presence of at least two populations of receptors. The association data identify with confidence two populations; the dissociation data suggest the presence of three or more populations. It is possible that dissociation experiments which do not require a "chase" of unlabeled EGF might occur with markedly different kinetics than dissociation in the presence of excess EGF. This could help to explain our observation of three dissociation rates in experiments with excess EGF. Development of methods to observe the dissociation of FITC-EGF in the absence of saturating concentration of mEGF will be required to characterize differences between EGF-induced dissociation rates and "intrinsic" dissociation rates.

Equilibrium Binding of FITC-EGF to EGF Receptor in A431 Membrane Vesicles. Examination of the binding of FITC-EGF to the EGF receptor in membranes under equilibrium conditions demonstrated that the equilibrium experiments were much less sensitive than kinetic experiments in distinguishing multiple classes of receptors. The anisotropy vs [FITC-EGF] plot for the equilibrium binding of FITC-EGF to EGF receptor in A431 membrane vesicles is shown in Figure 7. Both a one site and a two site model were used to fit these data (Figure 7, fit lines). For the fitting simulations, the r_{free} was fixed to 0.085 (determined in equilibrium control experiments), and the r_{bound} was set to 0.205 (obtained from the kinetic experiments). The one site model recovered a K_d = 0.84 nM (±0.37; SD), whereas the two site model obtained K_d's of 0.47 nM (unbounded, 1.8; SD) and 1.6 nM (±0.64). While our recovered K_d values were in good agreement with previously reported K_d values for the EGF receptor in A431 cell membranes using ^{125}I-EGF (Carraway et al., 1989; Berkers et al., 1990) and an FITC-EGF derivative (Carraway et al., 1990), completely unique values for the high affinity site and respective populations could not be obtained using exhaustive error analysis techniques (Beechem, 1992). The equilibrium data did demonstrate, however, that a two site model was required to adequately describe the data (75% confidence level, see Figure 7). Clearly, the equilibrium data were much less sensitive to the presence of multiple classes of receptors when compared to the kinetic experiments.

The higher sensitivity of kinetic measurements derives from their ability to detect rapid events in less populated states of the overall population that, at equilibrium, may be swamped out by the more highly populated states. In the case of EGF/receptor interactions, we observed very rapid binding to a high affinity subclass of receptor that was essentially complete in 10−20 s. Kinetically, this phase can be quantitated with very high accuracy, in terms of both rate constants and populations. In the equilibrium measurements, however, sensitivity to this receptor class is limited to observations at very low ligand concentrations, where measurements are intrinsically less accurate. In our study, equilibrium measurements indicate that some degree of heterogeneity exists, but the relative populations and their associated affinities cannot be uniquely determined from the data, i.e., the values obtained are statistically unbounded. The kinetic experiments can quantitate these populations and rate constants with a high level of confidence, i.e., with statistically well-defined upper and lower limits.

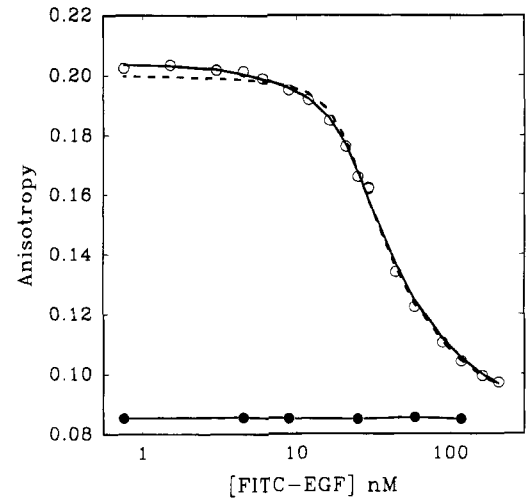

FIGURE 7: Equilibrium binding of FITC-EGF to EGF receptor in A431 membrane vesicles. This plot is the anisotropy vs [FITC-EGF] data from the equilibrium binding experiment (○) and the experimental control (●). This data were fit as described in Materials and Methods using a one site and two site model. The fits for the one site (- - -) and two site (—) models are shown with the data. The two site model fit is a better fit statistically; however, the small differences between the one and two site fits are indicative of the relative insensitivity of the equilibrium data in determining the presence of one or two affinity populations of EGF receptor.

ACKNOWLEDGMENT

We thank U. Barnella for technical assistance in preparation of mEGF and ^{125}I-mEGF, A. E. Kornegay for assistance with well culture and membrane preparation, Dr. C. A. Guyer for many helpful suggestions during the course of these studies, and Dr. A. H. Beth for helpful discussions and critical reading of the manuscript.

SUPPORTING INFORMATION AVAILABLE

Details of the preparation of A431 membrane vesicles, modifications to a Spex Fluorolog fluorometer for simultaneous acquistion of fluorescence and absorbance spectra, and a description of the T-format, steady-state fluorometer for monitoring the rapid anisotropy change in FITC-EGF upon binding to its receptor (4 pages). Ordering information is given on any current masthead page.

REFERENCES

Azevedo, J. R., & Johnson, D. A. (1990) *J. Membr. Biol. 118*, 215−224.

Beechem, J. M. (1992) *Methods Enzymol. 210*, 37−54.

Beechem, J. M., Gratton, E., Ameloot, M., Knutson, J. R., & Brand, L. (1991) in *Topics of Fluorescence Spectroscopy* (Lakowicz, J. R., Ed.) Vol. 2, pp 241−301, Plenum Press, New York.
Bellot, F., Moolenaar, W., Kris, R., Mirakhur, B., Verlaan, I., Ullrich, A., Schlessinger, J., & Felder, S. (1990) *J. Cell Biol. 110*, 491−502.
Berkers, J. A. M., van Bergen en Henegouwen, P. M. P., Verkleij, A. J., & Boonstra, J. (1990) *Biochim. Biophys. Acta 1052*, 453−460.
Berkers, J. A. M., van Bergen en Henegouwen, P. M. P., & Boonstra, J. (1992) *J. Recept. Res. 12*, 71−100.
Bloom, L., Otto, M., Eritja, R., Reha-Krantz, L., Goodman, M., & Beechem, J. M. (1994) *Biochemistry 33*, 7576−7586.
Böni-Schnetzler, M., & Pilch, P. F. (1987) *Proc. Natl. Acad. Sci. U.S.A. 84*, 7832−7836.
Buhrow, S. A., Cohen, S., & Staros, J. V. (1982) *J. Biol. Chem. 257*, 4019−4022.
Buhrow, S. A., Cohen, S., Garbers, D. L., & Staros, J. V. (1983) *J. Biol. Chem. 258*, 7824−7827.
Carpenter, G. (1985) *Methods Enzymol. 109*, 101−110.
Carpenter, G. (1987) *Annu. Rev. Biochem. 56*, 881−894.
Carpenter, G., & Cohen, S. (1976) *J. Cell Biol. 71*, 159−171.
Carpenter, G., & Cohen, S. (1990), *J. Biol. Chem. 265*, 7709−7712.
Carpenter, G., & Wahl, M. I. (1990) *Handb. Exp. Pharmacol. 95*, 69−171.
Carpenter, G., Lembach, K. J., Morrison, M. M., & Cohen, S. (1975) *J. Biol. Chem. 250*, 4297−4302.
Carpenter, G., King, L., Jr., & Cohen, S. (1979) *J. Biol. Chem. 254*, 4884−4891.
Carraway, K. L., III, & Cerione, R. A. (1993) *Biochemistry 32*, 12039−12045.
Carraway, K. L., III, Koland, R. A., & Cerione, R. A. (1989) *J. Biol. Chem. 264*, 8699−8707.
Carraway, K. L., III, Koland, R. A., & Cerione, R. A. (1990) *Biochemistry 29*, 8741−8747.
Cassel, D., & Glaser, L. (1982) *J. Biol. Chem. 257*, 9845−9848.
Chen, W. S., Lazar, C. S., Poenie, M., Tsien, R. Y., Gill, G. N., & Rosenfeld, M. G. (1987) *Nature 328*, 820−823.
Cochet, C., Kashles, O., Chambaz, E. M., Borrello, I., King, C. R., & Schlessinger, J. (1988) *J. Biol. Chem. 263*, 3290−3295.
Cohen, S., Ushiro, H., Stoscheck, C., & Chinkers, M. (1982) *J. Biol. Chem. 257*, 1523−1531.
Coker, K. J., Staros, J. V., & Guyer, C. A. (1994) *Proc. Natl. Acad. Sci. U.S.A. 91*, 6967−6971.
Defize, L. H. K., Boonstra, J., Meisenhelder, J., Kruijer, W., Tertoolen, L. G. J., Tilly, B. C., Hunter, T., van Bergen en Henegouwen, P. M. P., Moolenaar, W. H., & de Laat, S. W. (1989) *J. Cell Biol. 109*, 2495−2507.
Fabricant, R. N., DeLarco, J. E., & Todaro, G. J. (1977) *Proc. Natl. Acad. Sci. U.S.A. 74*, 565−569.
Fanger, B. O., Stephens, J. E., & Staros, J. V. (1989) *FASEB J. 3*, 71−79.
Faulkner-O'Brien, L. A., Beth, A. H., Papayannopoulos, I. A., Anjaneyulu, P. S. R., & Staros, J. V. (1991) *Biochemistry 30*, 8976−8985.
Gates, R. E., & King, L. E., Jr. (1982) *Mol. Cell. Endocrinol. 27*, 263−276.
Ghiron, C. A., Eftink, M. R., Engler, D. A., & Niyogi, S. K. (1992) *Photochem. Photobiol. 55*, 29−34.
Gill, G. N., Bertics, P. J., & Santon, J. B. (1987) *Mol. Cell. Endocrinol. 51*, 169−186.
Girard, D. J., Aaronsen, S. A., Todaro, G. J., Arnstein, P., Kersey, J. H., Dosik, H., & Parks, W. P. (1973) *J. Natl. Cancer Inst. 51*, 1417−1421.
Haigler, H., Ash, J. F., Singer, S. J., & Cohen, S. (1978) *Proc. Natl. Acad. Sci. U.S.A. 75*, 3317−3321.
Haigler, H. T., McKanna, J. A., & Cohen, S. (1979) *J. Cell Biol. 81*, 382−395.
Honegger, A. M., Szapary, D., Schmidt, A., Lyall, R., van Obberghen, E., Dull, T. J., Ullrich, A., & Schlessinger, J. (1987) *Mol. Cell. Biol. 7*, 4568−4571.
Johnson, M. L., & Frasier, S. G. (1985) *Methods Enzymol. 117*, 301−342.
Kawamoto, T., Sato, J. D., Le, A., Polikoff, J., Sato, G. H., & Mendelson, J. (1983) *Proc. Natl. Acad. Sci. U.S.A. 80*, 1337−1341.
Kienhuis, C. B. M., Heuvel, J. J. T. M., Ross, H. A., Swinkels, L. M. J. W., Foekens, J. A., & Benraad, T. J. (1991) *Clin. Chem. 37*, 1749−1755.
Kienhuis, C. B. M., Heuvel, J. J. T. M., Ross, H. A., Foekens, J. A., & Benraad, T. J. (1992) *Clin. Chem. 38*, 681−686.
King, A. C., & Cautrecasas, P. (1982) *J. Biol. Chem. 257*, 3053−3060.
Kohda, D., & Inagaki, F. (1992) *Biochemistry 31*, 11928−11939.
Laemmli, U. K. (1970) *Nature (London) 227*, 680−685.
Mayo, K. H., Nunez, M., Burke, C., Starbuck, C., Lauffenburger, D., & Savage, C. R. (1989) *J. Biol. Chem. 264*, 17838−17844.
McKanna, J. A., Haigler, H. T., & Cohen, S. (1979) *Proc. Natl. Acad. Sci. U.S.A. 76*, 5689−5693.
Montelione, G. T., Wüthrich, K., Burgess, A. W., Nice, E. C., Wagner, G., Gibson, K. D., & Scheraga, H. A. (1992) *Biochemistry 31*, 236−249.
Moolenaar, W. H., Bierman, A. J., Tilly, B. C., Verlaan, I., Defize, L. H. K., Honegger, A. M., Ullrich, A., & Schlessinger, J. (1988) *EMBO J. 7*, 707−710.
Otto, M. R., Lillo, M. P., & Beechem, J. M. (1994) *Biophys. J. 67*, 2511−2521.
Perez-Howard, G. M., Weil, P. A., & Beechem, J. M. (1995) *Biochemistry 34*, 8005−8017.
Rousseau, D. L., Jr. (1993) Ph.D. Dissertation, Vanderbilt University.
Rousseau, D. L., Jr., Staros, J. V., & Beechem. J. M. (1993) *Biophys. J. 64*, A385.
Savage, C. R., Jr., & Cohen, S. (1972) *J. Biol. Chem. 247*, 7609−7611.
Scatchard, G., (1949) *Ann. N.Y. Acad. Sci. 51*, 660−672.
Schlessinger, J., Schechter, Y., Willingham, M. C., & Pastan, I. (1978) *Proc. Natl. Acad. Sci. U.S.A. 75*, 2659−2663.
Staros, J. V., Fanger, B. O., Faulkner, L. A., Palaszewski, P. P., & Russo, M. W. (1989) in *Receptor Phosphorylation* (Moudgil, V. K., Ed.) pp 227−242, CRC Press, Boca Raton, FL.
Taylor, J. M., Mitchell, W. M., & Cohen, S. (1972) *J. Biol. Chem. 247*, 5928−5934.
Ullrich, A., & Schlessinger, J. (1990) *Cell 61*, 203−212.
Ullrich, A., Coussens, L., Hayflick, J. S., Dull, T. J. Gray, A., Tam, A. W., Lee, J., Yarden Y., Libermann, T. A., Schlessinger, J., Downward, J., Mayes, E. L. V., Whittle, N., Waterfield, M. D., & Seeburg, P. H. (1984) *Nature 309*, 418−424.
Ushiro, H., & Cohen, S. (1980) *J. Biol. Chem. 255*, 8363−8365.
van Bergen en Henegouwen, P. M. P., Defize, L. H. K., de Kroon, J., van Damme, H., Verkleij, A. J., & Boonstra, J. (1989) *J. Cell. Biochem. 39*, 455−465.
Walker, F., & Burgess, A. W. (1991) *J. Biol. Chem. 266*, 2746−2752.
Waters, C. M., Oberg, K. C., Carpenter, G., & Overholser, K. A. (1990) *Biochemistry 29*, 3563−3569.
Weber, G. (1992) *Protein Interactions*, p 16, equation 50, Chapman and Hall, London.
Wiegant, F. A. C., Blok, F. J., Defize, L. H. K., Linnemans, W. A. M., Verkelij, A. J., & Boonstra, J. (1986) *J. Cell Biol. 103*, 87−94.
Wolfsy, C., Goldstein, B., Lund, K., & Wiley, H. S. (1992) *Biophys, J. 63*, 98−110.
Yarden, Y., & Schlessinger, J. (1987a) *Biochemistry 26*, 1434−1442.
Yarden, Y., & Schlessinger, J. (1987b) *Biochemistry 26*, 1443−1451.
Zhou, M., Felder, S., Rubinstein, M., Hurwitz, D. R., Ullrich, A., Lax, I., & Schlessinger, J. (1993) *Biochemistry 32*, 8193−8198.

BI9513259